ACS OMEGA

http://pubs.acs.org/journal/acsodf

Article

Experimental Study on the Cement-Based Materials Used in Coal Mine Gas Extraction for Hole Sealing

Jianhua Fu, Dengke Wang,* Xuelong Li,* Zhiming Wang, Zhengjie Shang, Zhigang Jiang, Xiaobing Wang, and Xin Gao

Cite This: *ACS Omega* 2021, 6, 21094−21103

Read Online

ACCESS | Metrics & More | Article Recommendations

ABSTRACT: Gas drainage is an important method to prevent and control gas disasters. Sealing materials have an important impact on the gas drainage effect. To improve the extraction rate, the configuration and related characteristics of sealing materials were studied in this study. It was found that the fluidity increased gradually with the increase of the dosage of the suspension concentrate (SC). The water−cement ratio was directly proportional to the setting time of the slurry. Also, the mixing amount of the special cement was inversely proportional to the setting time of the slurry. The influence of the amount of foaming agent, special cement, and suspending agent on the expansion rate of the slurry was positive, and the influence gradually weakened. When the water−cement ratio of cement-based materials was 0.6, the special cement content percentage was 6, the suspension agent content percentage was 3, the plasticizer content percentage was 0.7, the early strength agent content percentage was 1.2, and the foaming agent content percentage was 0.2, the sealing effect was the best. The research results suggest that the porosity and pore length of the cement-based material are smaller than those of polyurethane, and its sealing property was better. This could further increase the sealing effect of the gas borehole, thereby facilitating gas extraction.

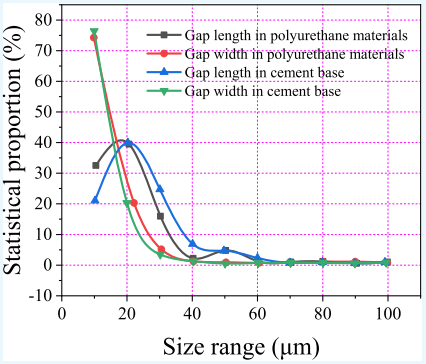

1. INTRODUCTION

Coal has been the main energy pillar in China, which has supported the rapid development of the national economy.[1−4] At present, 11.67% of the world's usable coal reserves are stored in China, ranked third in the world.[5−7] China is the largest coal-producing country in the world. Due to the deterioration of the environment and the emergence of various new energy sources, the proportion of coal in the consumption structure of primary energy has been reduced by the state's macrocontrol policies. However, the appearance of new energy is not enough to alleviate the current energy shortage problem.[8−11]

Currently, the number of coal mines with high gas content and coal and gas outburst is increasing.[12−15] In the process of coal production, coal mine gas accidents always threaten the safety of coal mines. The total number of coal mine deaths in China accounts for about 70% of the coal mine deaths in the world. Thus, the prevention and control of gas accidents is an important task needed to enhance the efficiency and reduce the risk of coal mine production.[16−18] The most effective method of coal mine gas control is gas drainage.[19−21] The gas drainage is required to reduce the coal seam gas content, gas pressure, and other indicators and then to achieve the requirements of safety production. The low-permeability coal seems to account for more than 95% of the coal seams mined in mines with high gas content and coal and gas outburst in China. The ultimate purpose of gas drainage hole sealing is to effectively use the negative pressure of gas drainage, to reduce the leakage of external air to the minimum, and then to improve the concentration of the drainage pipeline.[22−24] The quality of the sealing hole is directly related to the quality of the gas drainage effect, and the influence of sealing material on the gas drainage effect is very important. At the moment, the common sealing method is to employ polyurethane sealing material,[25−27] while the effect of this sealing method is very unstable. This is because the initial gas drainage concentration of a few boreholes can reach more than 90%, the gas drainage concentration of a few boreholes can reach more than 20%, and the gas drainage concentration of most boreholes in the later stage is only about 5−15%.[28−30] Due to the influence of temperature, man-made activities, hole collapse, and other factors, it is difficult to insert the polyurethane sealing material into the predetermined sealing depth of the drilling hole. Thus, foamed polyurethane cannot form enough expansion force and cannot squeeze the polyurethane into the cracks around the

Received: June 3, 2021
Accepted: July 23, 2021
Published: August 3, 2021

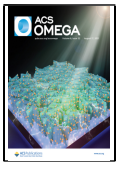

Table 1. Experiment Design

	influencing factors					
level	water−cement ratio	special cement (%)	suspending agent (%)	plasticizer (%)	early strength agent (%)	foaming agent (%)
1	0.55	4	2	0.6	1	0.1
2	0.6	5	3	0.7	1.1	0.15
3	0.65	6	4	0.8	1.2	0.2
4	0.7	7	5	0.9	1.3	0.25
5	0.75	8	6	1	1.4	0.3

hole in the sealed section.[31−33] Therefore, these cracks become air leakage channels. Moreover, as a small tunnel, the deformation and creep will inevitably occur in the case of in situ stress and excavation interference.[34,35] The foamed polyurethane has great elasticity and compressibility, and the hardness of the foamed polyurethane is far smaller than that of the coal rock, which cannot effectively support the borehole shape. This results in the continuous formation of cracks around the borehole in the sealed section after the hole sealing (the gas leakage channel is in the second stage).[36−39]

The polyurethane sealing method has the following problems:[40,41] (1) Polyurethane sealing strength at both ends is low. (2) The demand for ordinary cement is large and the labor intensity of workers is high. (3) Ordinary cement often has a certain shrinkage after solidification. Thus, it is easy to have an air leakage channel formed on the borehole wall. The use of a hole sealer for gas drainage hole sealing simplifies the underground hole sealing process and reduces the labor intensity of the sealing workers. There are many types of sealing equipment,[42−44] such as water pressure sealing device, air pressure sealing device, push expansion type hole sealing device, etc. No matter what type of sealing technology is used, the selection of sealing materials for gas drainage is the same strictly. Many experts and scholars have carried out extensive and in-depth research on sealing materials.[45−47] Based on their composition, sealing materials can be divided into three categories: inorganic materials (clay materials, cement-based materials, high-water materials, PD materials (a new hole sealing material), organic materials (polyurethane composite materials, carbon fiber (CF) materials, polyurethane polyurea materials), and flexible paste material (it is based on fly ash, with the water-retaining agent, expansion agent, cellulose, and coupling agent as auxiliary composite materials). Cement-based grouting material is widely used as sealing material for the time being. However, the ordinary cement material has the characteristics of shrinkage after solidification.[48−50] Adding a certain amount of admixtures into cement materials can improve the performance of cement. This improvement is obtained by reducing the hydration heat of materials, which improves the shrinkage characteristics of cement in the later stage, reduces the setting time of cement, improves the early strength of cement, increases the fluidity of cement, and improves the expansion characteristics of cement in the hydration process.[51−53]

To improve the sealing quality of drilling holes, experimental research was carried out in this study on the proportion of cement-based materials to obtain more suitable sealing materials for coal mines. The optimal ratio was determined mostly from the aspects of material fluidity, setting time, compressive strength, and expansion rate to improve the sealing effect and quality and to enhance the gas drainage efficiency.

2. EXPERIMENTAL DESIGN

Based on the theoretical analysis of the sealing hole and the actual operation situation, the best sealing effect can be obtained only when the grouting materials meet the following general requirements: stability, expansibility, and injectability. Their stability is reflected through the strength characteristics and long-term nonshrinkage. Thus, the material has to have a certain strength to ensure that the sealing material does not lose stability and is not damaged in the process of drilling-induced deformation and extrusion. Moreover, due to material shrinkage, the borehole sealing is not tight, resulting in air leakage. Therefore, the material is required to have a long-term nonshrinkage property. The expansion performance of the material depends on the expansion rate and the expansion force. Good expansibility not only can avoid leaving a "half-moon" gas leakage channel after grouting but also can provide certain active support for the borehole wall to compact loose coal around the borehole wall and to reduce the area of air leakage ring. The injectability suggests that the slurry can maintain good fluidity within a certain time to ensure the sealing grouting operation. During the operation, the slurry is injected into the sealing equipment and the predetermined position of the grouted section in the drilling.

Therefore, to study the comprehensive influence of different water−cement ratios and additives such as special cement, suspending agent, plasticizer, early strength agent, and foaming agent on the fluidity, setting time, and expansion rate of slurry, the orthogonal test method[54,55] was used. The aim was to analyze the influence and function of each component to fully realize the advantages of various additives, optimize the slurry performance, and enhance the sealing of boreholes' gas drainage effect. To reflect the influence of each factor on the slurry and to accurately represent the influence law, six factors and five levels were employed for the orthogonal test. The influencing factors and levels are shown in Table 1. L25 (56) test table was used, and its configuration is shown in the table.

3. EXPERIMENTAL RESULTS AND DISCUSSION

3.1. Fluidity of Grouting Sealing Material. *3.1.1. Liquidity Measurement Method.* The fluidity test of grouting materials was carried out by the flow test model.[56] The size of the truncated cone round mold was as follows: The inner diameter of the upper opening was $\Phi = 36 \pm 0.5$ mm, and the inner diameter of the lower opening was $\Phi = 61 \pm 0.5$ mm. Initially, the prepared slurry was put into the truncated cone mold, then scraped with a scraper, and lifted vertically and gently. Ultimately, the maximum diameter and vertical diameter of the slurry bottom were measured with a caliper, and the average value was calculated as an integer. Each fluidity test should be completed within 1 min.

3.1.2. Fluidity Measurement Results. According to the results of the orthogonal test, the water−cement ratio and the

https://doi.org/10.1021/acsomega.1c02911
ACS Omega 2021, 6, 21094−21103

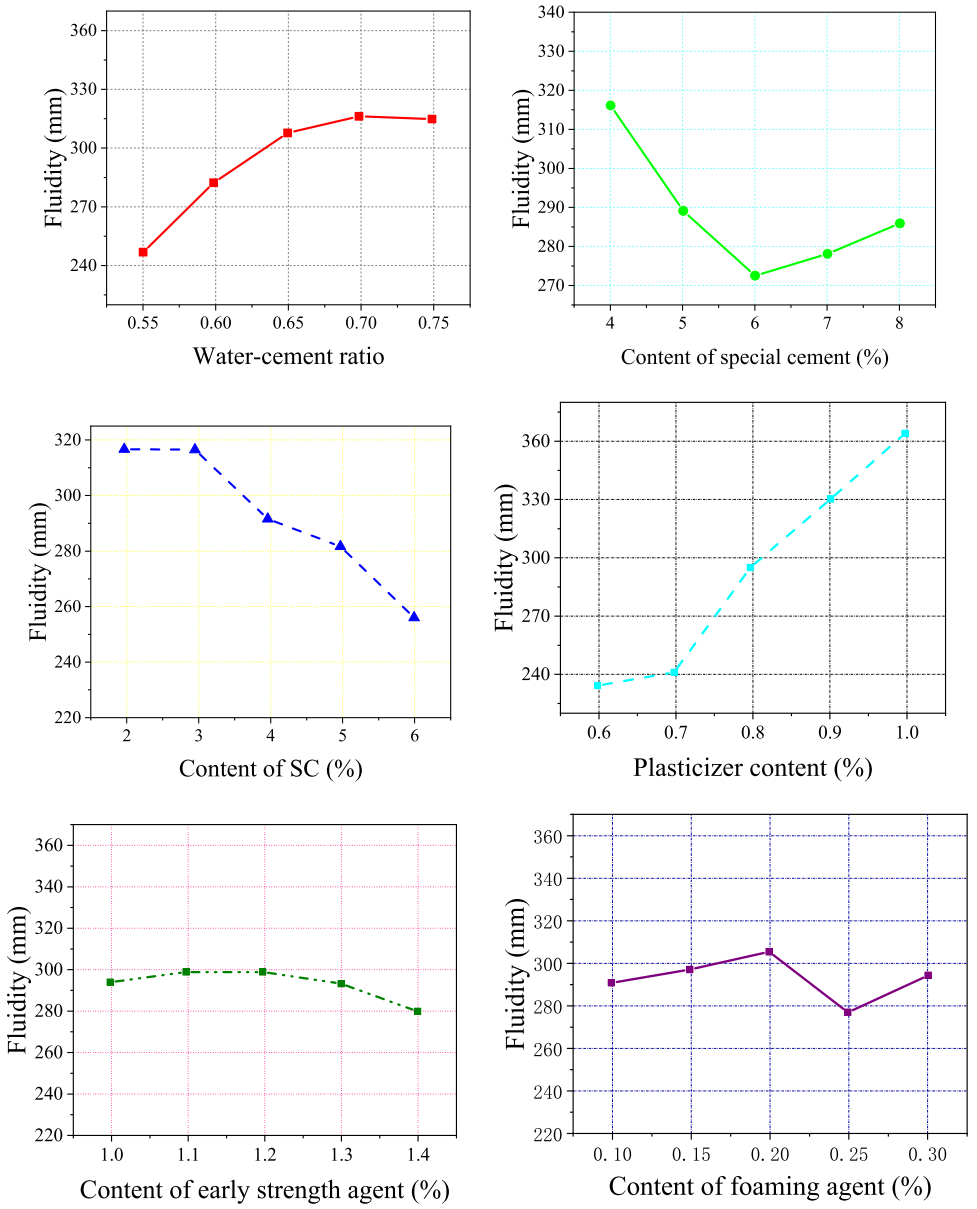

Figure 1. Effect curve of material fluidity.

proportion of each component influenced the fluidity of the material. The variation law of the fluidity is shown in Figure 1.

The effect of the early strength agent and foaming agent on the fluidity of slurry was not great, and the fluidity was about 280 mm (Figure 1). With the increase in the water−cement ratio and plasticizer content, the fluidity also increased gradually. However, the increase in the water−cement ratio was easy to cause water−cement separation of slurry. This was because the water ratio was far beyond the water required for cement hydration. Hence, fluidity increased significantly. The reason why the increase of plasticizer content could increase the fluidity was that it could reduce the amount of water used for slurry mixing. It could also adsorb and wrap on the surface of cement particles. These prevented the hydration reaction of cement, reduced the formation of hydration products, and then diminished the viscosity of the slurry and made the slurry denser. However, when the plasticizer content was greater than or equal to 0.8%, the slurry segregated when the water−cement ratio was greater than or equal to 0.6. With the increase in the amount of special cement, the fluidity first decreased and then increased. The minimum value was 271.8 mm, which met the requirements of injectability. The fluidity reduced with the increase of the content of suspension concentrate (SC) because the SC was very hygroscopic. Furthermore, the SC dispersed into a gelled or suspended state in the water medium. This could prevent the slurry from segregation, thereby increasing the slurry viscosity and reducing the fluidity.

3.2. Setting Time of Grouting Sealing Material.

3.2.1. Determination Method of Setting Time. According to GB/T1346-2011, the "test method for water consumption, setting time, and stability of cement net propeller consistency", the setting time of the material was measured by the Vicat instrument. The measuring device is exhibited in Figure 2. The time interval from the completion of slurry preparation to the initial setting of the slurry was considered as the initial setting time of slurry material. Furthermore, the time from the completion of slurry configuration to the final setting of slurry material was recorded as the final setting time of slurry

https://doi.org/10.1021/acsomega.1c02911
ACS Omega 2021, 6, 21094−21103

Figure 2. Vicat: setting time measuring device. 1: Vicat instrument; 2: initial setting test needle; 3: final coagulation test needle; 4: round mold.

material. After the preparation of the slurry, it was poured into the round mold, and the first measurement was conducted 30 minutes later. The test method was as follows: the round mold was put under the test needle, the contact between the test needle and the material surface was diminished, and finally, the test needle was suddenly released and vertically entered the material. When the test needle was 4 ± 1 mm away from the bottom plate, the slurry material reached the initial setting state. The determination method of the final setting time of the slurry was as follows: turn over the round mold immediately after the initial setting of the material, turn 180° and place the larger diameter side upward, and use the final coagulation test needle. When the accessory ring of the final setting needle cannot leave traces on the surface of the material, the material reaches the final setting state.

3.2.2. Determination of Setting Time. Figure 3 shows the setting time effect curve of the slurry.

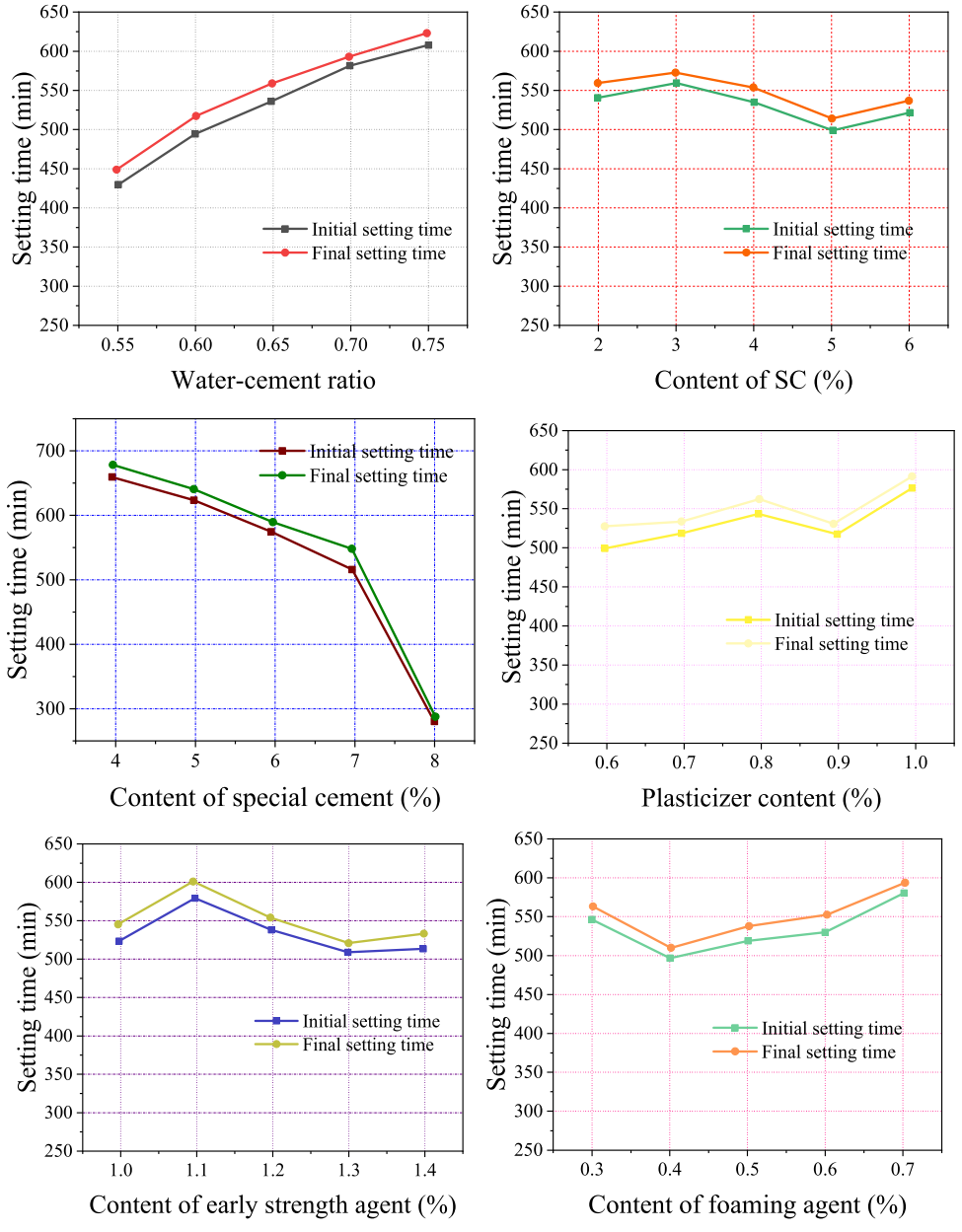

Figure 3. Setting time effect curve.

https://doi.org/10.1021/acsomega.1c02911
ACS Omega 2021, 6, 21094−21103

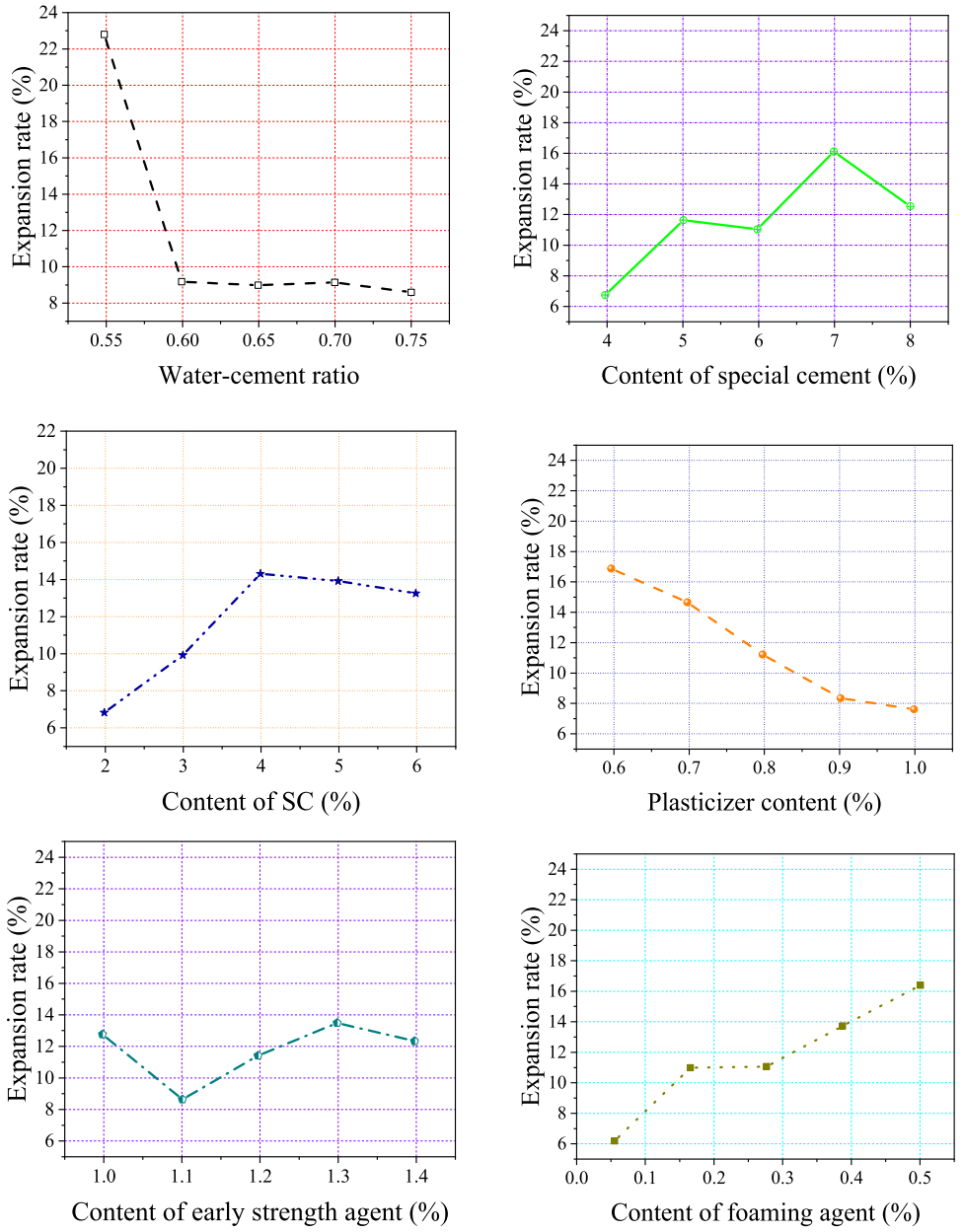

Figure 4. Expansion rate effect curve of the material.

It can be observed that the different amounts of the suspending agent, plasticizer, early strength agent, and the foaming agent had little impact on the setting time of slurry. The shortest initial setting time was 8.23 h and the longest was 9.63 h. The shortest final setting time was 8.43 h and the longest was 9.98 h. The final setting time was not more than 0.5 h after the initial setting. After the initial setting time of the slurry became 1.4 times longer than that of the initial setting of water, which achieved the fastest rate of 437.4 times of the initial setting time, the time did not exceed 11 h. During the test, when the water−cement ratio was greater than or equal to 0.6, scum was formed on the surface of the slurry of individual tests after solidification, which could be broken by pressing it through the finger. This was because the water content exceeded the water required for cement hydration, resulting in slurry segregation and inconsistent density between upper and lower grouts. The mixing amount of special cement was inversely proportional to the setting time of the slurry. The reason was that the special cement was very hydraulic. It could not only participate in the hydration reaction and reduce the mixing water but also had an early strength. The longest initial setting time was 2.35 times the shortest one. The longest final setting time was 2.35 times the shortest one, and the fastest final setting time was 4.67 h. The setting time effect curve of special cement indicated that when the content of special cement was smaller than or equal to 7%, the setting time diminished slowly with the increase of the special cement content. However, when the content of special cement was larger than 7%, the setting time was fast with the increase of the special cement content. The decrease in velocity was followed by a sudden increase in the change rate of the setting time.

3.3. Expansion Rate of Grouting Sealing Material. *3.3.1. Determination Method of the Expansion Rate.* The material expanded under the restriction of a plastic cup. The drainage method was applied to measure the expansion rate.

https://doi.org/10.1021/acsomega.1c02911
ACS Omega 2021, 6, 21094−21103

Table 2. Four Optimized Matching Parameters

number	water−cement ratio	special cement ratio	suspending agent	plasticizer	early strength agent	foaming agent	expansion rate (%)	mobility (mm)	initial setting time (min)	final coagulation time (min)
1	0.6	6	3	0.6	1.2	0.2	214	531	548	16
2	0.6	6	3	0.7	1.2	0.2	269	544	552	18
3	0.6	6	4	0.6	1.2	0.2	283	529	537	12.7
4	0.6	6	4	0.7	1.2	0.2	274	549	555	11.7

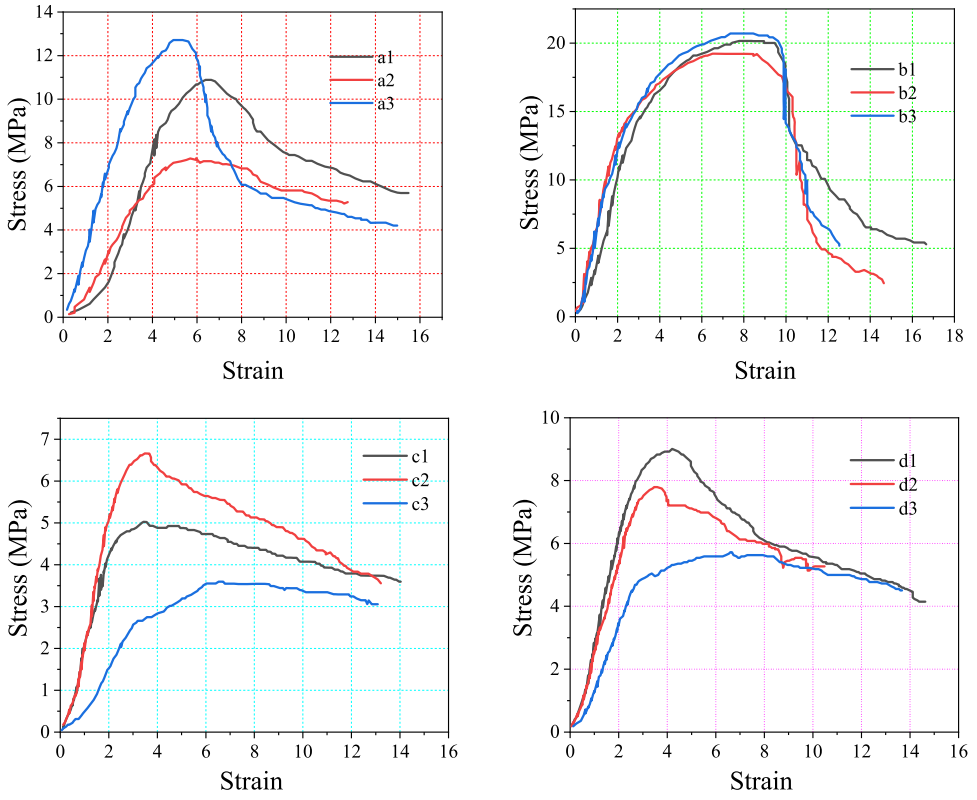

Figure 5. Stress−strain curves for different optimized matching parameters.

Although the deficiency of this method was that the expansion of the material was not completely free, the constraints of each group of material specimens were the same. Therefore, the measured data could also reflect the expansion properties of materials with different proportions. The volume of the plastic cup used was V_0 = 150.3 mL. The volume of the material after 28 days of expansion was determined by the drainage method. The specific method was as follows: the solidified material was taken out of the plastic cup, then its mass (M_1) was measured, and finally, its mass (M_2) was measured again after evenly coating by paraffin. The difference between the two masses was the mass (Δm) of the paraffin coated. This allowed us to further determine the volume (V_s) of the paraffin. When the volume measured in water was V_1, the expansion amount of the material was $V_1 - V_0 - V_s$, and the expansion rate of the material was $(V_1 - V_0 - V_s)/V_0 \times 100\%$.

3.3.2. Test Results of the Expansion Rate. Figure 4 indicates the expansion rate effect curve of the material.

Figure 4 shows that when the water−cement ratio was greater than or equal to 0.6, the water content had no significant influence on the expansion rate of the slurry, which was stable at about 9%. When the water−cement ratio was 0.55, the expansion rate was as large as 22.66%. Since the porosity of the material was large, the strength was reduced. At the same time, the excessive expansion was unfavorable to the hole sealing device and gas drainage hole. It caused a lot of unnecessary obstacles against the hole sealing technology. The change of the early strength agent did not cause the large fluctuation of the expansion rate of slurry. The minimum expansion rate was 8.48% when the amount of early strength agent was 1.1%, and the maximum value was 12.5% when the amount was 1%, which was 1.48 times the minimum expansion amount. When the content of the foaming agent was 0.3%, the maximum expansion rate was 16.28%. When the content of the foaming agent was 0.1%, the minimum expansion rate was 6.12%, and the maximum expansion rate was 2.66 times the minimum value. When the ratio was less than 1, it was a Bingham fluid, which had both viscosity and cohesive force. Therefore, a part of the gas generated by the foaming agent in the alkaline environment was sealed in the solidified material before it could be released. Thus, the expansion of the material was also a reason for the increase in porosity. When the content of special cement was 7%, the maximum expansion rate was 16.14%. When it was 4%, the minimum expansion rate was 6.64%, and the maximum expansion rate was 2.43 times the minimum value. The influence of special cement on the expansion rate of the slurry was caused by ettringite generated in the hydration process. The influence factors of special

https://doi.org/10.1021/acsomega.1c02911
ACS Omega 2021, 6, 21094−21103

cement on the setting time of slurry are illustrated in Figures 1, 3, and 4. They indicated that with the increase in the special cement amount, the setting time of slurry was shortened and more gas was generated. The body was sealed by the solidification of the slurry.

When the content of SC was 4%, the maximum expansion rate was 14.12%, and when the content of SC was 2%, the minimum expansion rate was 6.74%. The SC had hygroscopicity and expansibility. It provided a basic environment for the foaming agent. The maximum expansion rate was 16.68% when the content of the plasticizer was 0.6%. The minimum expansion rate was 7.48% when the amount of plasticizer was 1.67 times the minimum value, and the maximum expansion rate was 2.23 times the minimum expansion rate. This was because the sulfonic acid group with a negative charge was ionized in the solution of plasticizer, which combined with positive calcium ion and absorbed rapidly. It was attached to the surface of cement particles and wrapped with cement particles, which slowed down the hydration of cement to ettringite.

4. DETERMINATION OF THE MATERIAL RATIO

Based on the above study, the proportion of materials could be selected. Since the slurry was employed for sealing holes in gas drainage, the fluidity and expansion rate of slurry were considered as the main indexes, and the setting time of the slurry was taken as the secondary index. The fluidity and expansion rate could be as large as possible such that the sealed section could be saturated with materials to achieve the purpose of plugging the borehole. The initial setting time should not be too short to have enough time to be completed in construction. Moreover, the final setting time should not be too long to be set and hardened as soon as possible after sealing the hole. Therefore, four types of mixing ratios were selected preliminarily (Table 2).

4.1. Compressive Strength Characteristics Using Different Optimized Matching Parameters. Based on the ratio determined by the above tests, and in accordance with the requirements of the society of rock mechanics and engineering, the compressive strength of the specimens with a diameter of 50 × 100 mm^2 was tested. The stress−strain curves of four kinds of optimized matching parameters are displayed in Figure 5.

Figure 5 reveals that the stress of different materials increased with the increase of strain, while it reached the peak gradually and then declined. Besides, all four materials showed strong plastic behavior and no obvious brittle behavior. Compared with other types of matching, no. 2 material had the largest peak stress, about 20 MPa, and the minimum discreteness and strong heterogeneity, thus, no. 2 material was chosen. This material had the following characteristics:

(1) It could meet the requirements of bag grouting hole sealing, and the slurry did not flow out after the bag was injected.
(2) The flow time was controllable, and the solidification speed could be adjusted based on the tunnel temperature.
(3) The calorific value was small during the solidification process. It could expand about 18% after the later solidification.
(4) The initial strength was about 8 h, and it was not less than 4 MPa.

4.2. Dilatational Force Characteristic. After solidification, the sealing material could effectively reduce the cross-sectional area of the air leakage ring. Hence, it was of great significance to study the expansion force of the material. The self-developed expansion force test device was utilized in the test.

The expansion force of the no. 2 material was tested. The changing trend of expansion force with time is presented in Figure 6.

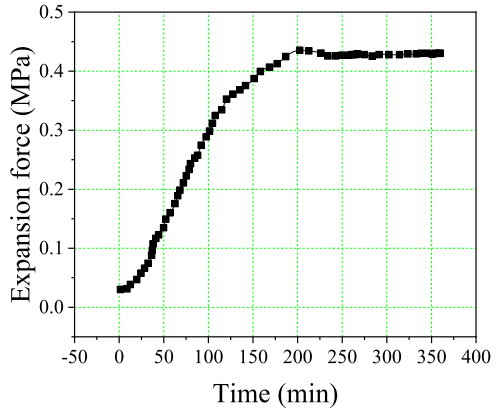

Figure 6. Expansion force−time curve of cement-based materials.

Figure 6 displays that the expansion force of cement-based materials first increased with time and then tended to become a constant value. Its stable expansion force value remained at 0.43 MPa after 4 h. It did not decay for a long time, which indicated that the material had experienced no shrinkage. Because of its expansive force, the material had a long-term supporting effect on the borehole, which had a positive effect on the tight sealing of the borehole.

4.3. Microstructural Characteristics. The development of the pores (including pores and fissures) in the sealing materials also affects the sealing performance of the materials. If the pores of the materials are developed, the air leakage channels are formed between the borehole wall and the materials. This results in the air leakage of the borehole. Therefore, scanning electron microscopy (SEM) experiments were carried out on the no. 2 materials and common polyurethane materials. The microscopic images of the materials are illustrated in Figure 7. The void ratio of the materials was analyzed by the digital processing technology, and the pore size was predicted.

After statistical analysis of the data calculated by the software, 117 voids were selected in the SEM images of polyurethane materials and 90 voids in the SEM images of cement-based materials. The results demonstrated that the porosity of polyurethane materials was 7.2%, and that of cement-based materials with no. 2 ratio was 5.6%. Figure 8 displays the distribution characteristics of the voids.

Figure 8 reveals that the gap length of the two materials was mostly concentrated in the range of 10−30 μm. Also, the maximum probability of the gap length between 11 and 15 μm was 37% in polyurethane materials and 35% in cement-based materials with gap length between 11 and 15 μm. Moreover, nearly 75% of the surface gap width of polyurethane materials and cement-based materials was distributed between 0 and 10 μm. Therefore, cement-based materials had better sealing performance than polyurethane materials.

https://doi.org/10.1021/acsomega.1c02911
ACS Omega 2021, 6, 21094−21103

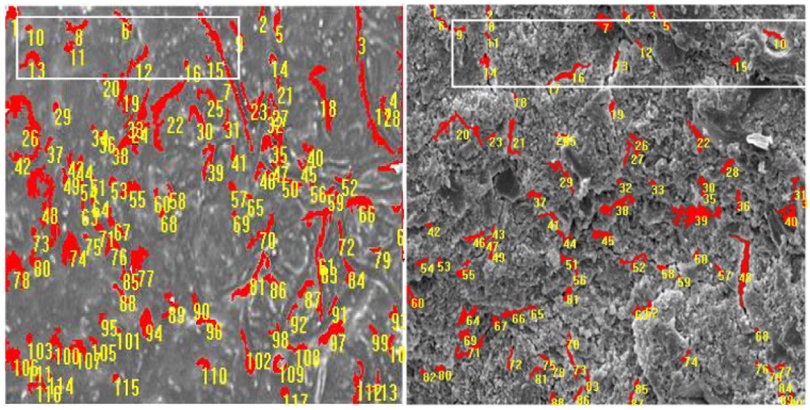

Figure 7. Graphic digital processing of materials by SEM.

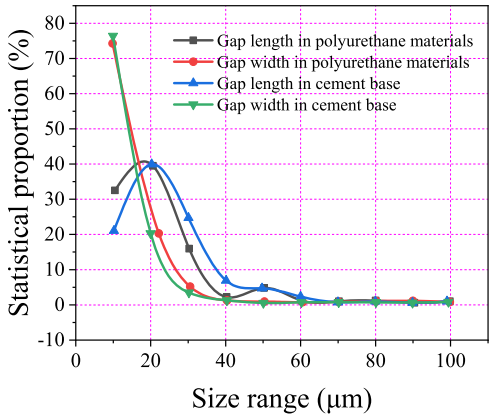

Figure 8. Void distribution characteristics.

Mine gas extraction is a major means of gas control, and "hole sealing" is an important technique in mine gas extraction. The soft coal seam's difficult drilling, sealing hole serious leakage, and technical problems such as nonstandard borehole coupling seriously affect the mine gas extraction. Through research and development of the new sealing hole grouting material, it is conducive to further combine the new hole sealing technology and hole sealing equipment, and then form the sealing technology suitable for the soft coal seam. In this way, we can achieve the comprehensive purpose of increasing the concentration, improving the extraction efficiency, reducing the sealing cost, and providing support for gas control and gas utilization.

5. CONCLUSIONS

The research mainly studied the materials used in gas drainage from the aspects of ratio, fluidity, setting time, expansion rate, compressive strength, microstructure, and other aspects. The main conclusions are summarized as follows:

(1) The effect of early strength agent and foaming agent on the fluidity of slurry was not significant. With the increase in water−cement ratio and plasticizer content, the fluidity increased gradually. However, the increase in water−cement ratio easily caused the water−cement of slurry to separate, and the fluidity to decrease with the increase of suspension agent content.

(2) The water−cement ratio was directly proportional to the setting time of the slurry. Furthermore, the mixing amount of the special cement was inversely proportional to the setting time of the slurry. The influence of the amount of the foaming agent, special cement, and suspending agent on the expansion rate of the slurry was positive. This influence was gradually weakened.

(3) Based on the compressive strength test, the best ratio of cement-based materials was as follows: water−cement ratio of 0.6, special cement content percentage of 6, suspending agent content percentage of 3, plasticizer content percentage of 0.7, early strength agent content percentage of 1.2, and foaming agent content percentage of 0.2. Its heat value was small in the process of solidification and could expand about 18% after later solidification.

(4) The results indicated that the expansion force of cement-based materials first raised and then tended to become a constant value. The initial strength was formed for about 8 h, and it was not smaller than 4 MPa. The porosity of cement-based materials was 5.6%, and the gap length between 11 and 15 μm was 35%, suggesting that the sealing property of cement-based materials was better.

AUTHOR INFORMATION

Corresponding Authors

Dengke Wang − *School of Safety Science and Engineering, Henan Polytechnic University, Jiaozuo 454000 Henan, China*; Email: wdk@hpu.edu.cn

Xuelong Li − *State Key Laboratory of Mining Disaster Prevention and Control and College of Energy and Mining Engineering, Shandong University of Science and Technology, Qingdao 266590 Shandong, China*; orcid.org/0000-0003-2037-2525; Email: lixlcumt@126.com

Authors

Jianhua Fu − *School of Safety Science and Engineering, Henan Polytechnic University, Jiaozuo 454000 Henan, China; Zhengzhou Coal Industry (Group) Corporation Limited Liability Company, Zhengzhou 450000 Henan, China*

Zhiming Wang − *School of Energy and Science Engineering, Henan Polytechnic University, Jiaozuo 454000 Henan, China*

Zhengjie Shang − *School of Safety Science and Engineering, Henan Polytechnic University, Jiaozuo 454000 Henan, China; Zhengzhou Coal Industry (Group) Corporation Limited Liability Company, Zhengzhou 450000 Henan, China*

Zhigang Jiang − *Sichuan Coal Industry Group Limited Liability Company, Chengdu 610091 Sichuan, China*

https://doi.org/10.1021/acsomega.1c02911
ACS Omega 2021, 6, 21094−21103

Xiaobing Wang − *Sichuan Coal Industry Group Limited Liability Company, Chengdu 610091 Sichuan, China*
Xin Gao − *College of Energy and Mining Engineering, Shandong University of Science and Technology, Qingdao 266590 Shandong, China*

Complete contact information is available at: https://pubs.acs.org/10.1021/acsomega.1c02911

Notes

The authors declare no competing financial interest.

■ ACKNOWLEDGMENTS

This work is supported by the National Natural Science Foundation of China (51774118), the Outstanding Youth Funds of Henan Polytechnic University (J2018-1), the Research Fund of the State Key Laboratory of Coal Resources and Safe Mining, CUMT (SKLCRSM19KF008), Taishan Scholars Project, Taishan Scholar Talent Team Support Plan for Advantaged & Unique Discipline Areas, Natural Science Foundation of Chongqing, China (cstc2019jcyj-bsh0041), Key R&D Plan of Shandong Province (2019SDZY034-2), and Postdoctoral Science Foundation Project Funded by State Key Laboratory of Coal Mine Disaster Dynamics and Control (2011DA105287-BH201903). The authors thank anonymous reviewers for their comments and suggestions to improve the manuscripts.

■ REFERENCES

(1) Chen, S. J.; Du, Z. W.; Zhang, Z.; Hua, W. Z.; Zhi, G. X.; Fan, F. Effects of chloride on the early mechanical properties and microstructure of gangue-cemented paste backfill. *Constr. Build. Mater.* **2020**, *235*, No. 117504.
(2) Han, W.; Tao, S.; Hou, L.; Yao, J. Geochemical characteristics and genesis of oil-derived gas in the Jingbian gas field, Ordos Basin, China. *Energy Fuels* **2017**, *31*, 10432−10441.
(3) Yan, F.; Xu, J.; Peng, S.; Zou, Q.; Li, Q.; Long, K.; Zhao, Z. Effect of capacitance on physicochemical evolution characteristics of bituminous coal treated by high-voltage electric pulses. *Powder Technol.* **2020**, *367*, 47−55.
(4) Fan, C. J.; Derek, E.; Li, S.; Chen, Z. W.; Luo, M. K.; Song, Y.; Zhang, H. H. Modelling and optimization of enhanced coalbed methane recovery using CO_2/N_2 mixtures. *Fuel.* **2019**, *253*, 1114−1129.
(5) Kong, B.; Wang, E. Y.; Lu, W.; Li, Z. Application of electromagnetic radiation detection in high-temperature anomalous areas experiencing coalfield fires. *Energy* **2019**, *189*, No. 116144.
(6) Kong, X. G.; Wang, E. Y.; Li, S. G.; Lin, H. F.; Zhang, Z. B.; Ju, Y. Q. Dynamic mechanical characteristics and fracture mechanism of gas-bearing coal based on SHPB experiments. *Theor. Appl. Fract. Mech.* **2020**, *105*, No. 102395.
(7) Li, X.; Cao, Z.; Xu, Y. Characteristics and trends of coal mine safety development. *Energy Sources, Part A* **2020**, *12*, 1−19.
(8) Liu, S.; Li, X.; Wang, D.; Zhang, D. Experimental study on temperature response of different ranks of coal to liquid nitrogen soaking. *Nat. Resour. Res.* **2021**, *30*, 1467−1480.
(9) Zhang, C. L.; Xu, J.; Yin, G. Z.; Peng, S. J.; Li, Q. X.; Chen, Y. X. A novel large-scale multifunctional apparatus to study the disaster dynamics and gas flow mechanism in coal mines. *Rock Mech. Rock Eng.* **2019**, *52*, 2889−2898.
(10) Xue, Y. C.; Sun, W. B.; Wu, Q. S. The influence of magmatic rock thickness on fracture and instability law of mining surrounding rock. *Geomech. Eng.* **2020**, *20*, 547−556.
(11) Zhang, R.; Liu, J.; Sa, Z. Y.; Wang, Z. Q.; Lu, S. Q.; Lv, Z. Y. Fractal characteristics of acoustic emission of gas-bearing coal subjected to true triaxial loading. *Measurement* **2020**, *169*, No. 108349.
(12) Liu, X. F.; Song, D. Z.; He, X. Q.; Wang, Z. P.; Zeng, M. G.; Wang, L. K. Quantitative analysis of coal nanopore characteristics using atomic force microscopy. *Powder Technol.* **2019**, *346*, 332−340.
(13) Fan, J. Y.; Chen, J.; Jiang, D. Y.; Wu, J. X.; Shu, C.; Liu, W. A stress model reflecting the effect of the friction angle on rockbursts in coal mines. *Geomech. Eng.* **2019**, *18*, 21−27.
(14) Fan, C. J.; Elsworth, D.; Li, S.; Chen, Z. W.; Luo, M. K.; Yu, S.; Zhang, H. H. Modelling and optimization of enhanced coalbed methane recovery using CO_2/N_2 mixtures. *Fuel* **2019**, *253*, 1114−1129.
(15) Li, H.; Zheng, C. S.; Lu, J.; Tian, L.; Lu, Y.; Ye, Q.; Luo, W.; Zhu, X. Drying kinetics of coal under microwave irradiation based on a coupled electromagnetic, heat transfer and multiphase porous media model. *Fuel* **2019**, *256*, No. 115966.
(16) Kong, B.; Liu, Z.; Yao, Q. G. Study on the electromagnetic spectrum characteristics of underground coal fire hazardous and the detection criteria of high temperature anomaly area. *Environ. Earth Sci.* **2021**, *80*, No. 89.
(17) Liu, X.; Zhang, H.; Wang, X.; Zhang, C.; et al. Acoustic emission characteristics of graded loading intact and holey rock samples during the damage and failure process. *Appl. Sci.* **2019**, *9*, No. 1595.
(18) Shen, W.; Shi, G.; Wang, M.; Rong, T.; et al. Method of entry layout under synergistic effects of abutment stress and dynamic stress. *Shock. Vib.* **2020**, *2*, No. 6655293.
(19) Zheng, C. S.; Jiang, B. Y.; Xue, S.; Chen, Z.; Li, H. Coalbed methane emissions and drainage methods in underground mining for mining safety and environmental benefits, A review. *Process Saf. Environ. Prot.* **2019**, *127*, 103−124.
(20) Zhang, D.; Cen, X. X.; Wang, W. F.; Deng, J.; Wen, H.; Xiao, Y.; Shu, C. M. The graded warning method of coal spontaneous combustion in Tangjiahui Mine. *Fuel* **2021**, *288*, No. 119635.
(21) Zou, Q. L.; Liu, H.; Cheng, Z. H.; Zhang, T. C.; Lin, B. Q. Effect of slot inclination angle and borehole-slot ratio on mechanical property of pre-cracked coal, Implications for ECBM recovery using hydraulic slotting. *Nat. Resour. Res.* **2020**, *29*, 1705−1729.
(22) Karacan, C. O.; Diamond, W. P.; Schatzel, S. J. Numerical analysis of the influence of in-seam horizontal methane drainage boreholes on longwall face emission rates. *Int. J. Coal Geol.* **2007**, *72*, 15−32.
(23) Yan, F.; Xu, J.; Peng, S.; Zou, B.; Zhou, B.; Long, K.; Zhao, Z. Breakdown process and fragmentation characteristics of anthracite subjected to high-voltage electrical pulses treatment. *Fuel* **2020**, *275*, No. 117926.
(24) Xue, Y.; Dang, F.; Liu, F.; Li, R. J.; Ranjjth, P. G.; Wang, S. H.; Cao, Z. Z.; Yang, Y. G. An elastoplastic model for gas flow characteristics around drainage borehole considering post-peak failure and elastic compaction. *Environ. Earth Sci.* **2018**, *77*, No. 669.
(25) Maya, I. D.; Weatherspoon, J.; Young, C. J.; Barker, J.; Allon, M. Increased risk of infection associated with polyurethane dialysis grafts. *Semin. Dial.* **2007**, *20*, 616−620.
(26) Jaunich, M.; Stark, W.; Wolff, D. Comparison of low temperature properties of different elastomer materials investigated by a new method for compression set measurement. *Polym. Test.* **2012**, *31*, 987−992.
(27) Mu, B.; Li, M. Fabrication and characterization of polyurethane-grafted reduced graphene oxide as solid-solid phase change materials for solar energy conversion and storage. *Sol. Energy* **2019**, *188*, 230−238.
(28) Zhang, T.; Bao, R.; Li, S.; Zhang, C.; Zhang, L. Expansion properties and creep tests for a new type of solidified expansive sealing material for gas drainage boreholes in underground mines. *Environ. Earth Sci.* **2018**, *77*, No. 468.
(29) Wang, Z.; Sun, Y.; Wang, Y. L.; Zhang, J. X.; Sun, Z. D. A coupled model of air leakage in gas drainage and an active support sealing method for improving drainage performance. *Fuel* **2019**, *237*, 1217−1227.

(30) Akgün, H.; Koçkar, M. K. Evaluation of a sand bentonite mixture as a shaft/borehole sealing material. *Appl. Clay Sci.* **2018**, *164*, 34−43.
(31) Fu, J. H.; Li, X. L.; Wang, Z. M. A novel sealing material and a bag-grouting sealing method for underground CBM drainage in China. *Constr. Build. Mater.* **2021**, *299*, No. 124016.
(32) Zhou, A. T.; Wang, K. A new inorganic sealing material used for gas extraction borehole. *Inorg. Chem. Commun.* **2019**, *102*, 75−82.
(33) Zhou, F.; Sun, W. B.; Shao, J. L.; Kong, L. J.; Geng, X. G. Experimental study on nano silica modified cement base grouting reinforcement materials. *Geomech. Eng.* **2020**, *20*, 67−73.
(34) Bagherian, A.; Shiraz, A. S. Flowable composite as fissure sealing material? A systematic review and meta-analysis. *Br. Dent. J.* **2018**, *224*, 92.
(35) Aghkand, Z. K.; Dil, E. J.; Ajji, A.; Dubois, C. Simulation of heat transfer in heat sealing of multilayer polymeric films, Effect of process parameters and material properties. *Ind. Eng. Chem. Res.* **2018**, *57*, 14571−14582.
(36) Wang, Y. Analysis of dynamic characteristics of through-wall cracks between 2 boreholes in the directed fracture controlled blasting. *Fatigue Fract. Eng. Mater. Struct.* **2018**, *41*, 273−286.
(37) Li, X. L.; Chen, S. J.; Wang, S.; et al. Study on in situ stress distribution law of the deep mine taking Linyi Mining area as an example. *Adv. Mater. Sci. Eng.* **2021**, *9*, No. 5594181.
(38) Simon, H.; Buske, S.; Krauß, F.; Giese, R.; Hedin, P.; Juhlin, C. The derivation of an anisotropic velocity model from a combined surface and borehole seismic survey in crystalline environment at the COSC-1 borehole, central Sweden. *Geophys. J. Int.* **2017**, *210*, 1332−1346.
(39) Wang, C.; Song, D. Z.; Zhang, C. L.; Liu, L.; Zhou, Z. H.; Huang, X. C. Research on the classification model of coal's bursting liability based on database with large samples. *Arabian J. Geosci.* **2019**, *12*, No. 411.
(40) Song, H. P.; Xie, W. S.; Liu, J. Q.; Cheng, F. Q.; Gasem, K. A. M.; Fan, M. H. Effect of surfactants on the properties of a gas-sealing coating modified with fly ash and cement. *J. Mater. Sci.* **2018**, *53*, 15142−15156.
(41) Sanches, A. O.; Teixeira, G. F.; Zaghete, M. A.; Longo, E.; Malmonge, J. A.; Silva, M. J.; Sakamoto, W. K. Influence of polymer insertion on the dielectric, piezoelectric and acoustic properties of 1-0-3 polyurethane/cement-based piezo composite. *Mater. Res. Bull.* **2019**, *119*, No. 110541.
(42) Zhang, Z. B.; Liu, X. N.; Zhang, Y. H.; et al. Comparative study on fracture characteristics of coal and rock samples based on acoustic emission technology. *Theor. Appl. Fract. Mech.* **2021**, *111*, No. 102851.
(43) Simon, K.; Porz, L.; Swamy, T.; Chiang, Y. M.; Slocum, A. Low-profile self-sealing sample transfer flexure box. *Rev. Sci. Instrum.* **2017**, *88*, No. 083705.
(44) Daemen, J. J. K. Borehole studies of rock engineering problems in large scale laboratory equipment. *Geophys. Res. Lett.* **1981**, *8*, 711−714.
(45) Ghanaati, S.; Willershausen, I.; Barbeck, M.; Unger, R. E.; Joergens, M.; Sader, R. A.; Kirkpatrick, C. J.; Willershausen, B. Tissue reaction to sealing materials, different view at biocompatibility. *Eur. J. Med. Res.* **2010**, *15*, 483−492.
(46) Bram, M.; Reckers, S.; Drinovac, P.; Monch, J.; Steinbrech, H. P.; Buchkremer, H. P.; Stover, D. Deformation behavior and leakage tests of alternating sealing materials for SOFCs stacks. *J. Power Sources* **2004**, *138*, 111−119.
(47) Li, X. L.; Chen, S. J.; Li, Z. H.; Wang, E. Y. Rockburst mechanism in coal rock with structural surface and the microseismic (MS) and electromagnetic radiation (EMR) response. *Eng. Failure Anal.* **2021**, *124*, No. 105396.
(48) Vangelatos, I.; Angelopoulos, G. N.; Boufounos, D. Utilization of ferroalumina as raw material in the production of ordinary Portland cement. *J. Hazard. Mater.* **2009**, *168*, 473−478.
(49) Iacobescu, R. I.; Angelopoulos, G. N.; Jones, P. T.; Blanpain, B.; Pontikes, Y. Ladle metallurgy stainless steel slag as a raw material in ordinary Portland cement production, a possibility for industrial symbiosis. *J. Cleaner Prod.* **2016**, *112*, 872−881.
(50) Tittarelli, F.; Mobili, A.; Chiara, G.; Belli, A.; Bellezze, T. Corrosion behaviour of bare and galvanized steel in geopolymer and Ordinary Portland Cement based mortars with the same strength class exposed to chlorides. *Corros. Sci.* **2018**, *134*, 64−77.
(51) Cao, J.; Chung, D. D. L. Microstructural effect of the shrinkage of cement-based materials during hydration, as indicated by electrical resistivity measurement. *Cem. Concr. Res.* **2004**, *34*, 1893−1897.
(52) Yang, R.; Sharp, J. H. Hydration characteristics of Portland cement after heat curing, I, Degree of hydration of the anhydrous cement phases. *J. Am. Ceram. Soc.* **2001**, *84*, 608−614.
(53) Chaei, M. G.; Akbarnezhad, A.; Castel, A.; Lloyd, R.; Keyte, L.; Foster, S. Precision of cement hydration heat models in capturing the effects of SCMs and retarders. *Mag. Concr. Res.* **2018**, *70*, 1217−1231.
(54) Zhao, C. W.; Chen, X. P.; Zhao, C. S. Study on CO_2 capture using dry potassium-based sorbents through orthogonal test method. *Int. J. Greenhouse Gas Control* **2010**, *4*, 655−658.
(55) Feng, F.; Chen, S. J.; Wang, Y. J.; Huang, W. P.; Han, Z. Y. Cracking mechanism and strength criteria evaluation of granite affected by intermediate principal stresses subjected to unloading stress state. *Int. J. Rock. Mech. Min.* **2021**, *143*, No. 104783.
(56) *GB/T 50080-2002, Standard for Test Method of Performance on Ordinary Fresh Concrete*; China Architecture and Building Press: Beijing, China, 2002.

https://doi.org/10.1021/acsomega.1c02911
ACS Omega 2021, 6, 21094−21103